Emergent phases in a discrete flocking model with non-reciprocal interaction

Matthieu Mangeat[1] Swarnajit Chatterjee[1,2] Jae Dong Noh[3] Heiko Rieger[1]

[1]Department for Theoretical Physics, Saarland University, Saarbrücken, Germany

[2]Laboratoire de Physique Théorique et Modélisation, CY Cergy Paris Université, Cergy, France

[3]Department of Physics, University of Seoul, Seoul, Korea

Abstract

Non-reciprocal interactions arise in systems that seemingly violate Newton's third law "actio=reactio". They are ubiquitous in active and living systems that break detailed balance at the microscale, from social forces to antagonistic inter-species interactions in bacteria. Non-reciprocity affects non-equilibrium phase transitions and pattern formation in active matter and represents a rapidly growing research focus in the field. In this work, we have undertaken a comprehensive study of the non-reciprocal two-species active Ising model [1], a non-reciprocal discrete-symmetry counterpart of the continuous-symmetry two-species Vicsek model. Our study uncovers a distinctive run-and-chase dynamical state that emerges under significant non-reciprocal frustration. In this state, A-particles chase B-particles to align with them, while B-particles avoid A-particles, resulting in B-particle accumulation at the opposite end of the advancing A-band. This run-and-chase state represents a non-reciprocal discrete-symmetry analog of the chiral phase seen in the non-reciprocal Vicsek model. Additionally, we find that self-propulsion destroys the oscillatory state obtained for the non-motile case.

Non-reciprocal two-species active Ising model

- N particles on a periodic square lattice with $L_x \times L_y$ sites. Average density: $\rho_0 = N/L_xL_y$.
- Equal population of both species: $N_A = N_B = N/2$.
- The j^{th} particle on site i is equipped with a spin-orientation $\sigma_i^j = \pm 1$.
- The j^{th} particle is further equipped with a species-spin $s_i^j = \pm 1$; $s_A = 1$, $s_B = -1$.
- No restriction is applied on the number of particles $\rho_i = \sum_{s,\sigma} n_{s,i}^{\sigma}$ on site i.
- Intra-species interactions: $J_{AA} = J_{BB} = J = 1$.
- Species A aligns with species B with an interaction strength J_{AB} ($0 \le J_{AB} \le J$).
- Species B anti-aligns with species A with interaction strength J_{BA} ($-J \le J_{BA} \le 0$).
- $J_{AB} = -J_{BA} = J_{NR} \le J$.
- Flipping rate for the spin-orientation (on-site) [2]:

$$W_{\text{flip}}^{\text{NR}}(\sigma \to -\sigma) = \gamma \exp\left(-\frac{2\beta_1}{\rho_i}\sigma\mu_s^{\text{eff}}\right).$$

- Effective local magnetization: $\mu_A^{\text{eff}} = J_{AA}m_A + J_{AB}m_B$, $\mu_B^{\text{eff}} = J_{BB}m_B + J_{BA}m_A$, $m_s = n_s^+ - n_s^-$.
- Dimensionless variables: $\beta_1 \equiv \beta J = T^{-1}$ and $\mathcal{J}_{ss'} = J_{ss'}/J$; $\gamma = 1$.
- Nearest-neighbor biased hopping in 1d ($\pm\mathbf{e}_x$) [const. hopping rate D along $\pm\mathbf{e}_y$] [2]:

$$W_{\text{hop}}(\sigma) = D(1 \pm \sigma\varepsilon); \quad 0 \le \varepsilon \le 1.$$

Time-evolution of the NRTSAIM at maximum non-reciprocity

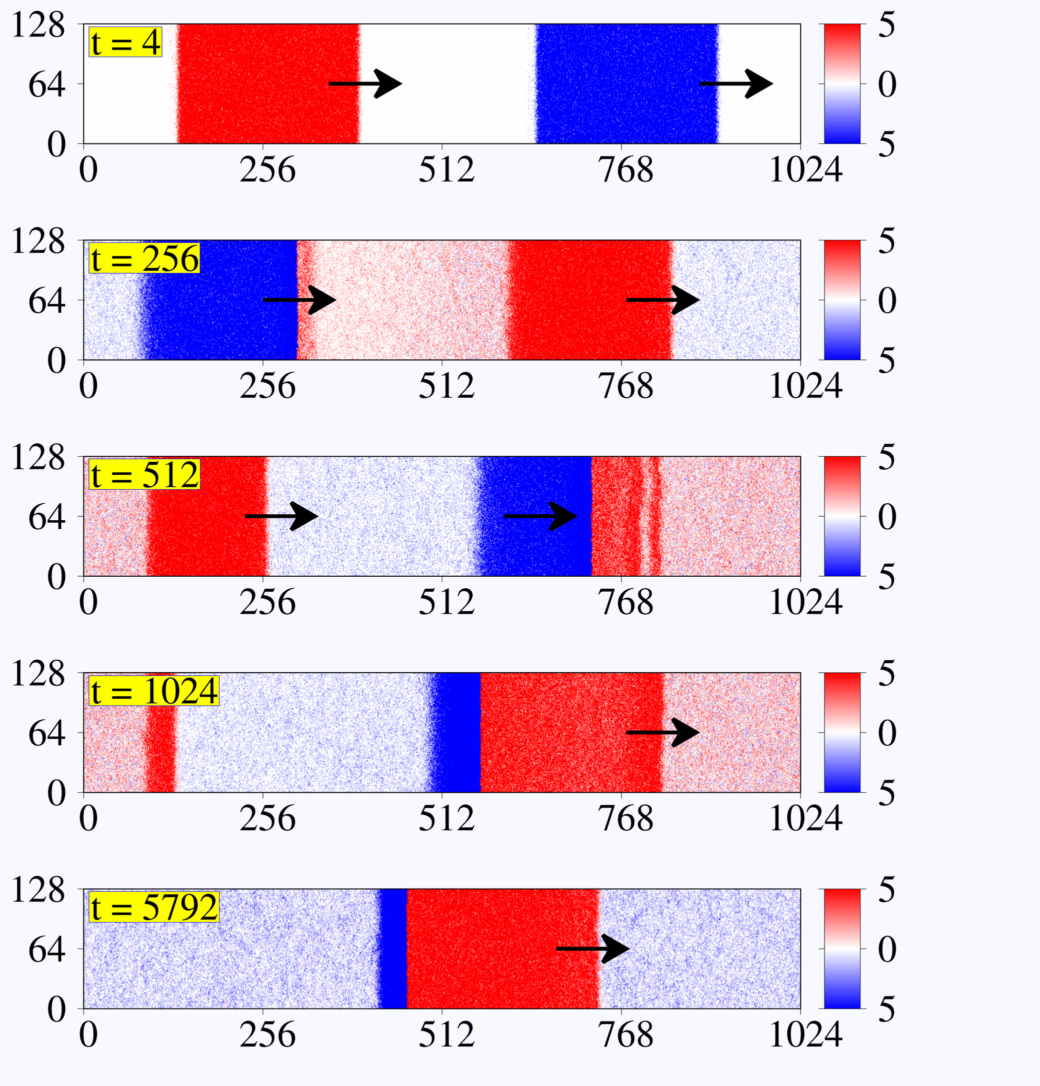

$\beta_1 = 1.25$, $\rho_0 = 4$, $\varepsilon = 0.9$ and $\mathcal{J}_{NR} = 1$

- **Coupled run-and-chase state**
- Red: Species A; Blue: Species B
- Nucleation of an A-band in the gas phase in front of the B-band ($t = 256$)
- To avoid them, B-particles start to accumulate ($t = 512, 1024$)
- Substantial accumulation → denser B-band and slowing down of band velocity ($t = 5792$)
- Allows B-particles to maintain maximum distance from pursuing A-particles

Steady-state snapshots and density profiles for various $\mathcal{J}_{NR}$

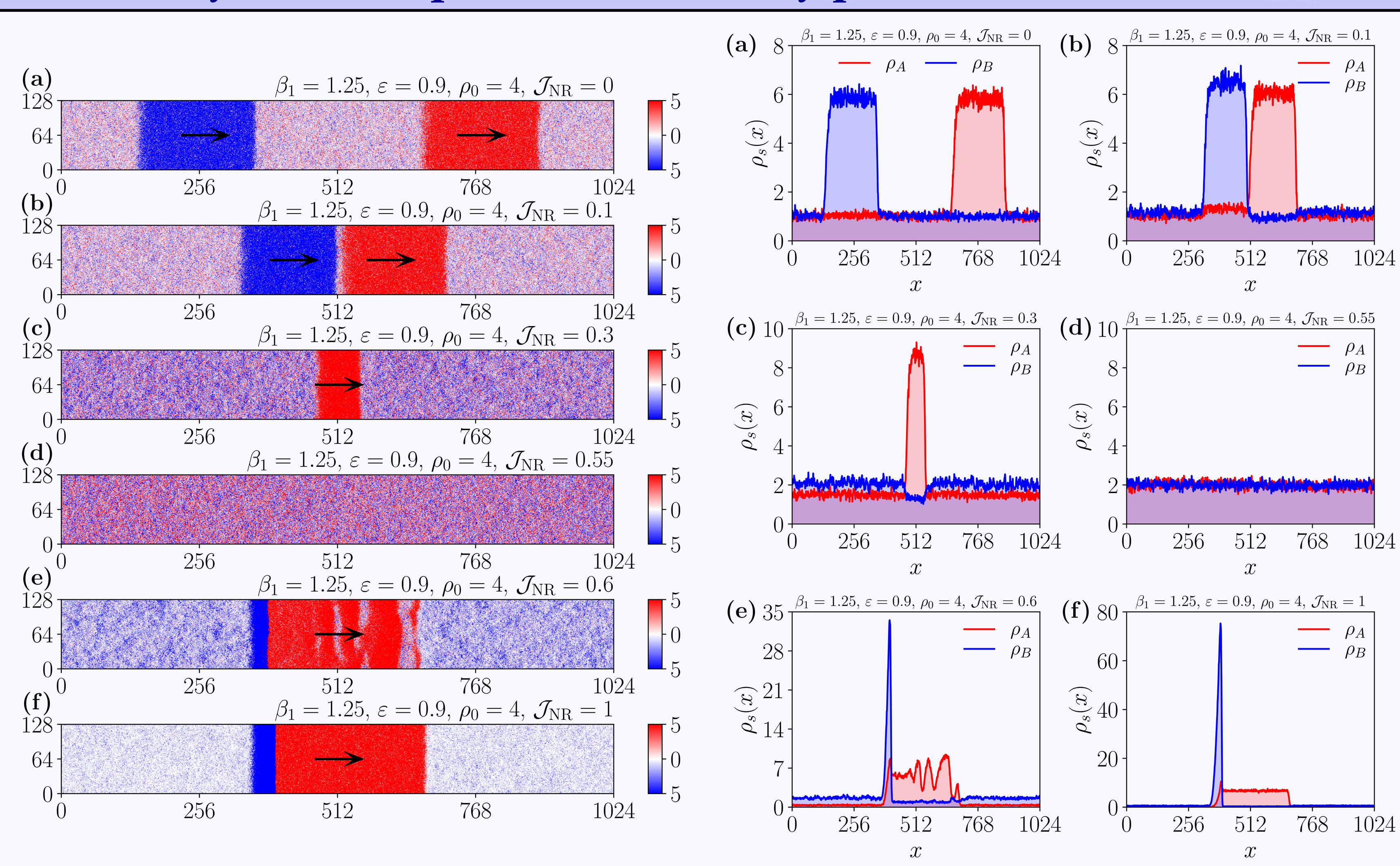

(a–b) band velocity $c \sim 1.96$ is larger than the self-propulsion velocity of the particles $v = 2D\varepsilon = 1.8$ for small $\mathcal{J}_{NR}$. (e–f) $c \sim 1.64$ of the B-band is smaller than v since the NR interaction slows down the B-band.

NRTSAIM State Diagrams

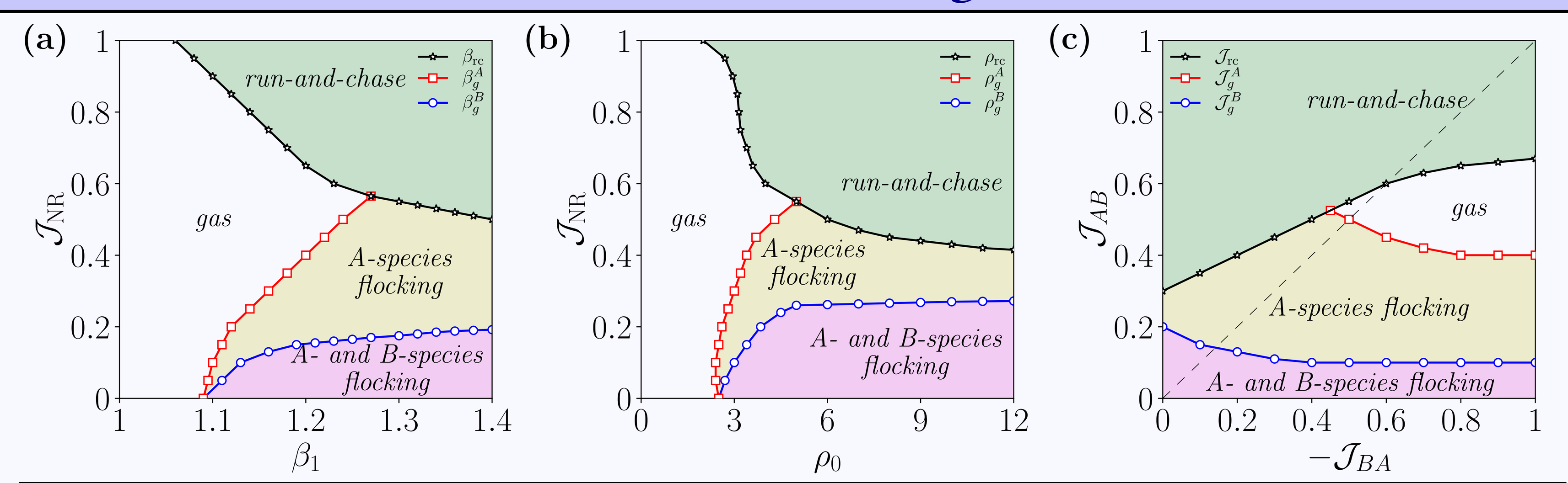

- (a) $\mathcal{J}_{NR} - \beta_1$ diagram for $\rho_0 = 4$, (b) $\mathcal{J}_{NR} - \rho_0$ diagram for $\beta_1 = 1.25$, and (c) $\mathcal{J}_{AB} - \mathcal{J}_{BA}$ diagram for $\beta_1 = 1.25$, $\rho_0 = 4$, and $\varepsilon = 0.9$.

Purely diffusive NRTSAIM ($\varepsilon = 0$)

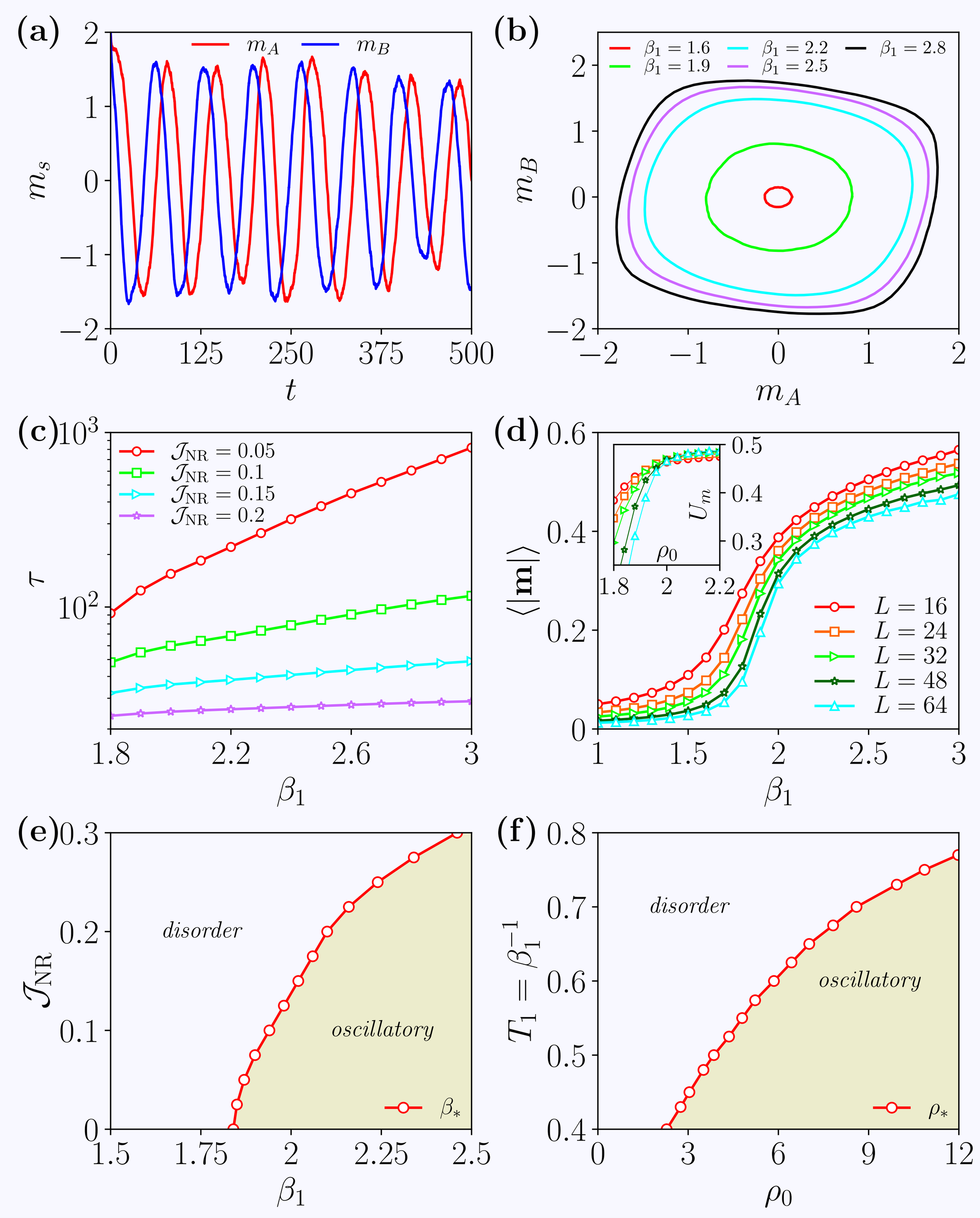

- (a) Time-evolution of m_A and m_B exhibits an oscillatory (swap) state. $\beta_1 = 2.2$, $\rho_0 = 4$, and $\mathcal{J}_{NR} = 0.1$.
- (b) System exhibits stable limit cycles. $\mathcal{J}_{NR} = 0.1$.
- (c) τ increases exponentially with β_1, and decreases with $\mathcal{J}_{NR}$.
- (d) $\mathbf{m} = (m_A, m_B)$ characterizes the transition between the disordered state and the oscillatory state.
- The transition occurs at $\beta_* = 1.94$.
- (e) $(\mathcal{J}_{NR}, \beta_1)$ state diagram for $\rho_0 = 4$. Disorder/oscillatory transition line corresponds to Hopf bifurcation.
- (f) (T_1, ρ_0) state diagram for $\mathcal{J}_{NR} = 0.1$.

Hydrodynamic equations of the NRTSAIM

- Average particle density $\rho_s^{\sigma}(\mathbf{x};t) \equiv \langle n_s^{\sigma}(\mathbf{x};t)\rangle$ in state σ and species s.
- Particle density $\rho_s(\mathbf{x};t) = \sum_\sigma \rho_s^{\sigma}(\mathbf{x};t)$ and the magnetization $m_s(\mathbf{x};t) = \sum_\sigma \sigma\rho_s^{\sigma}(\mathbf{x};t)$ of species s.
- Hydrodynamic equations:

$$\partial_t \rho_s = D\nabla^2\rho_s - v\partial_x m_s$$

$$\partial_t m_s = D\nabla^2 m_s - v\partial_x\rho_s + 2\gamma_s(\rho)\left[\left(\rho_s - \frac{r_{ss}}{2\beta_1\mathcal{J}_{ss}}\right)\sinh\left(\frac{2\beta}{\rho}J_{ss'}m_{s'}\right) - m_s\cosh\left(\frac{2\beta}{\rho}J_{ss'}m_{s'}\right)\right].$$

- Self-propulsion velocity $v = 2D\varepsilon$.
- $\gamma_s(\rho) = \gamma_{NR}\exp[(r_{sA} + r_{sB})/2\rho]$ and $r_{ss'} = (2\beta J_{ss'})^2\alpha_{s'}$.
- If we consider $\alpha_A = \alpha_B$ as well as $J_{AA} = J_{BB}$ for identical species but with non-reciprocal interactions, we get $r_{AA} = r_{BB} = r$, $r_{AB} = (J_{AB}/J)^2 r$ and $r_{BA} = (J_{BA}/J)^2 r$.

Results from solving the hydrodynamic equations

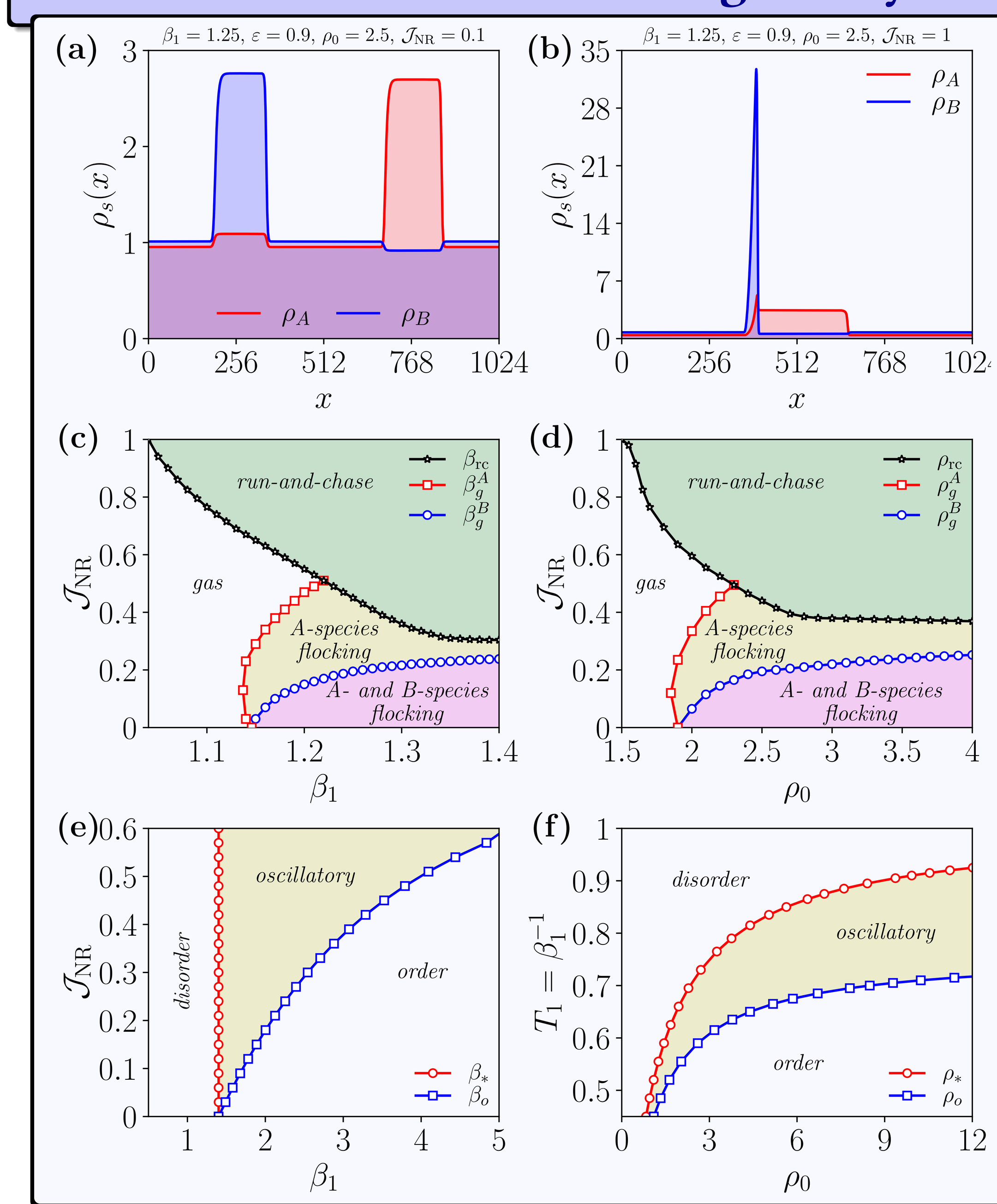

- Density profiles for (a) $\mathcal{J}_{NR} = 0.1$ and (b) $\mathcal{J}_{NR} = 1$. $\varepsilon = 0.9$.
- (c) $(\mathcal{J}_{NR}, \beta_1)$ state diagram for $\rho_0 = 2.5$ and $\varepsilon = 0.9$.
- (d) $(\mathcal{J}_{NR}, \rho_0)$ state diagram for $\beta_1 = 1.25$ and $\varepsilon = 0.9$.
- (e) $(\mathcal{J}_{NR}, \beta_1)$ state diagram for $\rho_0 = 2.5$ and $\varepsilon = 0$.
- (f) temperature-density state diagram for $\mathcal{J}_{NR} = 0.1$ and $\varepsilon = 0$.
- In our numerical simulations, we do not observe any ordered state for any nonzero values of $\mathcal{J}_{NR}$, even at large β_1.
- In numerical simulations of our microscopic model, the oscillatory state persists, likely because particles can still diffuse when $\varepsilon = 0$, which stabilizes the oscillatory state.

Summary

- The NRTSAIM exhibits a highly efficient run-and-chase state, where B-particles accumulate at the far end of the advancing A-band, maximizing their distance.
- In the non-motile NRTSAIM, for any nonzero $\mathcal{J}_{NR}$, regardless of how small, the oscillation period does not diverge at a finite temperature, showing that no ordered state can be reached.

References

[1] A. P. Solon and J. Tailleur, Phys. Rev. E **92**, 042119 (2015).

[2] M. Mangeat, S. Chatterjee, J. D. Noh, and H. Rieger, Commun. Phys. **8**, 186 (2025).

Acknowledgments

This work is financially supported by the German Research Fondation (DFG) within the Collaborative Research Center SFB 1027. Travel support for attending this conference is provided by CY Cergy Paris University, Cergy, France.

swarnajitchatterjee@gmail.com/ swarnajit.chatterjee@cyu.fr